# Dielectric Properties of Wall-Building Materials in Southeast Asia at 1.12-1.7 GHz

Narathep Phruksahiran

Department of Electrical Engineering, Chulachomklao Royal Military Academy, Nakhon Nayok, Thailand

narathepp@gmail.com

**Abstract.** *This paper presents a measurement-based analysis of the complex relative permittivity in typical construction walls in Southeast Asia, such as hollow clay brick and lightweight concrete, using the insertion transfer function methodology. A vector network analyzer performs the measurements between 1.12 GHz and 1.7 GHz, based on the standard rectangular waveguide WR-650 and the radar frequency in the L band at 1.3 GHz, to identify the construction frequency material's frequency and polarization dependence characteristics. The estimated complex relative permittivity in each polarization state (hh, hv, vh, vv) can be used to analyze further the wall type and the object detection behind the wall.*

**Received by** 29 December 2022
**Revised by** 24 February 2023
**Accepted by** **0**4 April 2023

## Keywords:

relative permittivity, insertion transfer function, frequency response, construction wall.

## 1. Introduction

Significant problems in communication technology and through the wall radar systems are related to building material properties. Therefore, there is an essential demand for an investigation on the materials used in modern and traditional construction. The Authors in [1, 2] reviewed the characteristics of the common materials used in structuring, such as brick, concrete, glass, and wood, in terms of measurement procedures and frequency-dependent response.

Because electromagnetic wave propagation and material properties are linked, it is crucial to investigate the material properties according to a specific frequency band and application. For instance, in determining propagation losses in the extended-spectrum band from 800 MHz to 8 GHz [3], research narrowed to the range of the 60 GHz band, which is required in each study depending on the common goal of employment [4], and focusing on the time delay estimation of backscattered signals from a wall [5].

Diverse processes and techniques applied to estimate the dielectric characteristics of distinct samples are the following: free space, two-terminal, time-domain, frequency-domain, closed cavity, dielectric probe, and waveguide techniques, for example, the measured the complex relative permittivity of substances in indoor conditions by practicing two open-ended coaxial probes [6]. Unfortunately, the bricks and concrete samples have to be sliced due to the equipment's limited dimension. [7, 8] performed a free-space measurement scheme suitable for nondestructive and contactless dielectric estimation of composite substance. The samples have not to be manufactured to match the measuring setup. They can be implemented to inhomogeneous elements and without contacting or damaging the structure. The analysis procedures typically commit to the time-domain strategy and the frequency-domain approach. Thus, for example, the narrowband frequency-domain measurement is derived from continuous-wave power estimation. On the other hand, the wideband frequency-domain measurement is accustomed to achieving the electromagnetic properties of construction material by sweeping toward the aspired frequency band. Time-domain-based determinations are based on the objective evaluation of reflected or refracted wave radiating from the material plate, depending on whether the measurement setup is organized in a reflection, as demonstrated by [9], or transmission geometry, as shown by [10]. Electromagnetic waves that interact with construction will provide losses that depend on the electrical characteristics of the building structure and material composition [11]. The methods used in the measurement are associated with the theory of transverse electromagnetic mode in lossy media and the theory of material electrical properties, which consist of attenuation constant, phase constant, wavelength, velocity, and skin depth [12]. Another essential variable is the orientation of the electric field intensity vector and the magnetic field intensity vector, or polarization, [13]. Furthermore, the complex permittivity of a material, its thickness, surface roughness, and the polarization and incident angle of electromagnetic waves determine the quantity of energy reflected and transmitted through it. The wall attenuation can be determined by measuring the received power, as demonstrated by [14-16], or by using the Fresnel reflection coefficients, as shown by [17, 18]. One successful approach is the characterization of the object based on the measured insertion transfer function, which is a widely used method for noncontact electromagnetic characterization of materials, as presented by [19-21]. This function defines the proportion of two phaser signals measured in the presence and absence of the material under inspection, as shown by [22]. In addition, several experimental characterizations based on free-space

techniques have been done recently by several authors. Still, the results are varied and depend on both experiment conditions and the composition of considered materials, [23].

The construction of walls is usually based on architectural and structural considerations. Even if the component's nature is known, their impact on electromagnetic waves is challenging to forecast. Therefore, it is crucial to investigate the properties of construction materials in each sector of the world. [24] performed the reflection coefficient measurement of the house flooring materials for North American House. The Authors in [25] have examined the experience of the behavior of radio propagation in the historic Italian town. Finally, [26] investigated the radio wave propagation of the brick wall in southern European construction.

To the author's best knowledge, there is no investigation of building material used in the South East Asian region. Moreover, the climate in this area is hot and humid, making the layout of the building structure and materials used in construction distinctive and have specific features. Therefore, this paper aims to empirically study the material properties of common constructive material in South East Asia at the L-Band frequency. The L-band frequencies are attractive because they are low and can travel through obstacles better than higher frequencies. It is furthermore widely used in radar systems. We utilize the insertion transfers functional and free-space techniques to determine the electromagnetic characteristics of hollow clay bricks (br) and lightweight concrete (lc).

The rest of this paper is organized as follows. First, Section 2 presents the system model and problem formulation. Then, the Experiment setup and the measurement procedures are described in Section 3. Next, Section 4 summarizes the estimation results for all frequencies in the 1.12-1.7 GHz (L-Band). Finally, Section 5 declares the conclusions.

## 2. System Model and Problem Formulation

The complex relative permittivity, symbolized by $\varepsilon_r = \varepsilon_r' - j\varepsilon_r''$ characterizes the material properties and is the basis for estimating the attenuation and dispersion of signal through the wall. The determination of complex relative permittivity consists of two steps. The first step is measuring of the insertion transfer function using the time-domain or frequency-domain techniques. This function compares the voltage signal in the free-space measurement condition, expressed by $v_f(t)$, and the voltage signal from the measurement through the material slab, symbolized by $v_m(t)$. The formulation of the insertion transfer function, denoted as $H(j\omega)$, is defined as:

$$H(j\omega) = \frac{\mathrm{FFT}(v_m(t))}{\mathrm{FFT}(v_f(t))} = \frac{V_m(j\omega)}{V_f(j\omega)} \quad (1)$$

where $\omega = 2\pi f$ is the angular frequency, FFT denotes the Fast Fourier Transform used to convert the sampled time-domain signals to the frequency domain data, represented by $V_f(j\omega)$ and $V_m(j\omega)$ for the free-space measurement and the measurement through material slab, respectively.

The second step is the evaluation of complex relative permittivity using the measured signal from equation (1). Under assuming that the wall and the antennas are adjusted, the direction of the incident plane wave is perpendicular to the wall. In the scattering terminology, the transmission coefficient T is analogous to the parameter $S_{21}$, which can be measured using a vector network analyzer. Based on the boundary conditions for electromagnetic fields at the slab-air interfaces, the estimation of the transmission coefficient T straightforwardly through the wall with thickness $d$ is $H(j\omega) = Te^{j\beta_0 d}$. According to [19], the insertion transfer function can be obtained as:

$$H(j\omega) = \frac{4e^{j\beta_0 d}}{e^{\gamma d}\left(2+\frac{\eta_0}{\eta}+\frac{\eta}{\eta_0}\right)+e^{-\gamma d}\left(2-\frac{\eta_0}{\eta}-\frac{\eta}{\eta_0}\right)} \quad (2)$$

where $\beta_0 = \omega\sqrt{\mu_0\varepsilon_0}$ , $\gamma = \alpha + j\beta = j\omega\sqrt{\mu_0\varepsilon_0(\varepsilon_r' - j\varepsilon_r'')}$, $\eta_0 = \sqrt{\mu_0/\varepsilon_0}$ , and $\eta = \eta_0/\sqrt{\varepsilon_r' - j\varepsilon_r''}$.

In the case of low loss material, with $\varepsilon_r''/\varepsilon_r' \ll 1$, the simplified solution of the equation based on one dimension root search techniques can be determined by numerically solving the following equation, as proved by [22]:

$$\tan[\beta_0 d - \angle H(j\omega)] + \frac{1-QX}{1+QX}\tan(\beta d) = 0 \quad (3)$$

where

$$\beta = \beta_0\sqrt{\varepsilon_r'} \quad (4)$$

$$Q = \left(\frac{\sqrt{\varepsilon_r'}-1}{\sqrt{\varepsilon_r'}+1}\right)^2 \quad (5)$$

$$X = e^{-2\alpha d} = \frac{K-\sqrt{K^2-(\varepsilon_r'-1)^4}}{\left(\sqrt{\varepsilon_r'}-1\right)^4} \quad (6)$$

and

$$K = \cos(2\beta d)(\varepsilon_r' - 1)^2 + 8\frac{\varepsilon_r'}{|H(j\omega)|^2} \quad (7)$$

After $\varepsilon_r'$ has been resolved, the imaginary part of the complex permittivity, $\varepsilon_r''$ and the loss tangent can be determined from:

$$\varepsilon_r'' = \frac{2c\alpha\sqrt{\varepsilon_r'}}{\omega} \quad (8)$$

where $c$ is the velocity of light in free-space.

## 3. Experimental Description

The measurement campaign was performed at the Department of Electrical Engineering of Chulachomklao Royal Military Academy, Thailand. An anechoic chamber was not available when performing these measurements. Instead, directional antennas with small beamwidth are

utilized to guarantee that only the distinct signal through the material was being measured and to withdraw or significantly decrease any diffraction effects nearby the edges of the material under study.

Fig, 1 represents the experimental setup for this study. The Keysight FieldFox RF Analyzer N9913A module, as shown in Fig. 1(a), was adapted to perform measurements by a sweeping signal in the frequency range from 1.12 GHz to 1.7 GHz (L-Band) with $\Delta f$ = 1.25 MHz in each measurement step. A PC can be connected to the N9913A through LAN for real-time data processing. In this work, the pyramidal horn antennas are designed with a gain of 12 dBi. They are specified for use with the frequency range from 1.12 GHz to 1.7 GHz based on the standard rectangular waveguide WR-650 configuration and are utilized for transmitting and receiving purposes. The Port 1 (RF Output) is fed through a 1.5 m cable (model: MHD142 RADIALL) to the transmitter (Tx) antenna mounted on a tripod. On another site of the measurement setup, an identical antenna mounted on a similar tripod is employed as the receiver (Rx) antenna. It is coupled to Port 2 (RF Input) through a 1.5 m cable, as depicted in Fig. 1(b) and (c), respectively.

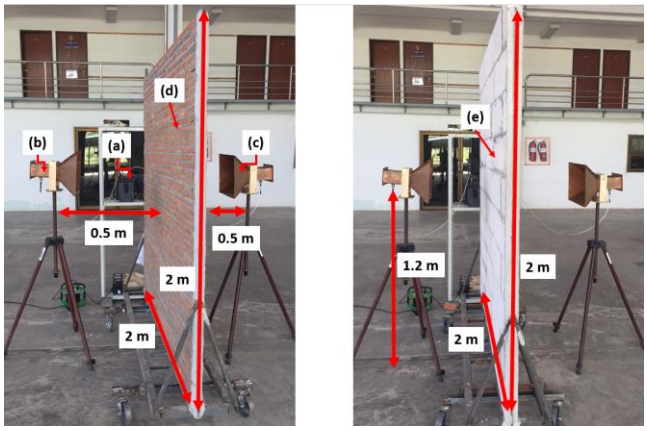


**Fig. 1** Measurement system setup.

This study considers two representations of the typical construction wall in Southeast Asia, such as hollow clay brick (br) and light-weighted concrete (lc), for the complex relative permittivity estimations. We employed the standardized hollow clay brick with 130 mm x 25 mm x 50 mm (length x height x thick). The dimension of each light-weighted concrete block is 600 mm x 200 mm x 75 mm (length x height x thick). All hollow clay bricks and light-weighted concrete blocks are laying in conventional horizontal orientation. The material can be assumed to be low loss and the singgle-pass techniques can be performed. The sample wall material is 2x2 m large suitable to cover the beam footprint of the incident wave, as shown in Fig. 1(d) and (e), respectively. The wall material is deposited precisely halfway within the antennas at 0.5 m from the antenna. Thus, the wall is in the far-field zone of the individual antenna, and the electromagnetic field on the surface is a plane wave. Applying this setting, we consider the hh, hv, vh, and vv polarization. The first letter in hh, hv, vh, and vv subscripts is the polarization of the transmitted wave. The second letter is of the polarization of the received wave. The indices h and v stand for horizontal and vertical polarization, which depends on the electric field's orientation to the plane of incidence, perpendicular, and parallel, respectively

## 4. Results and Discussion

The relative permittivity determinations were carried out for a couple of sample substances, i.e., a clay brick wall and a lightweight concrete wall. The properties of two different materials were determined using the data processing process earlier described. For particular materials, the measurements were accomplished in a transmission arrangement. The mean real part of complex relative permittivity and the loss tangent, including a confident standard deviation from the measurement data and the complex equations in the frequency range between 1.12 and 1.7 GHz, are analyzed and summarized in Table 1. Fig. 2 presents the magnitude of $S_{21}$ obtained from the measurements, Fig. 3 illustrates the comparison of the calculated real part of complex relative permittivity $\varepsilon_r'$, Fig. 4 displays the comparison of the estimated imaginary part of complex relative permittivity $\varepsilon_r''$, of each sample wall depending on polarization.

In detail, Table 1 shows the average real part of the relative permittivity and the loss tangent over the 1.12 - 1.7 GHz frequency range, including their standard deviation in each polarization state. From the table, the difference between the permittivity values of the two experimental materials, i.e., clay brick and lightweight concrete, is observable, including the effects arising from the incidence of the electric field. From the results of this experiment, it can be concluded that bricks have a higher permittivity than lightweight concrete. Moreover, The hh polarization delivers a lower permittivity in clay brick with $\varepsilon_r'$ = 4.5323. In lightweight concrete, a lower permittivity can be found in vv polarization with $\varepsilon_r'$ = 2.3869.

| Pol. | Mat. | $\boldsymbol{\varepsilon_r'}$ | std. | $\boldsymbol{\tan(\delta)}$ | std. |
|---|---|---|---|---|---|
| hh | br | 4.5323 | 0.2583 | 0.0026 | 0.0003 |
| hh | lc | 2.4504 | 0.1031 | 0.0045 | 0.0005 |
| hh | br | 4.9071 | 0.4352 | 0.0026 | 0.0004 |
| hh | lc | 2.4066 | 0.2175 | 0.0046 | 0.0007 |
| vv | br | 4.8826 | 0.5453 | 0.0025 | 0.0004 |
| vv | lc | 2.5276 | 0.3294 | 0.0044 | 0.0008 |
| vv | br | 5.0800 | 0.2359 | 0.0025 | 0.0003 |
| vv | lc | 2.3869 | 0.0942 | 0.0046 | 0.0006 |

**Table 1** The Average Relative Permittivity And The Loss Tangent Over The Frequency Range 1.12-1.7 GHz.

Fig. 2 demonstrates the magnitude of $S_{21}$ acquired from the experiments in dB compared between the measurement in free space (fs-hh, fs-hv, fs-vh, and fs-vv), the propagation through the brick wall (br-hh, br-hv, br-vh, and br-vv), and by using the lightweight concrete (lc-hh, lc-hv, lc-vh, and lc-vv) as obstacle medium. From the graph, it can be seen that the magnitude of $S_{21}$ tends

to decrease as the frequency increases, as expected. Furthermore, there were significant differences when altering the experimental material and the position of the electric field. This graph characteristic will lead to calculations using Equation (1) correctly based on differences of the measurement in free space and by using the material slab. It also describes the properties of the wall in response to frequency over the 1.12 - 1.7 GHz range.

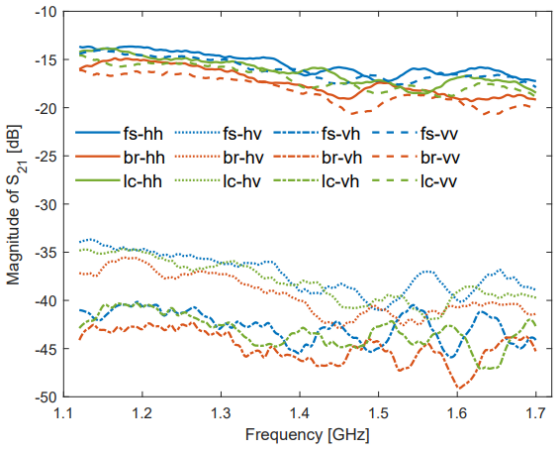


**Fig. 2** Frequency and polarization dependence of the measured $S_{21}$.

Fig. 3 and Fig. 4 display the frequency and polarization dependence of the estimated real part, $\varepsilon_r'$, and imaginary part, $\varepsilon_r''$, of the complex permittivity, respectively. However, as shown in Table 1, the average permittivity in different polarization states is comparable. The line curves are relatively consistent across the frequency range in hh and vv polarization, which can be applied to compare and use with a wideband signal. But in the frequency range between 1.4 - 1.7 of hv and vh polarization, it can be seen that the character of the graph fluctuates and can affect the signal when used in this frequency band.

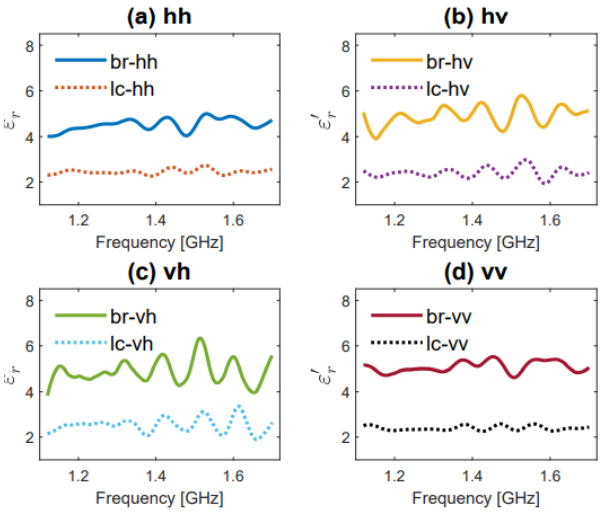


**Fig. 3** Frequency and polarization dependence of the estimated real part of the complex permittivity, $\varepsilon_r'$.

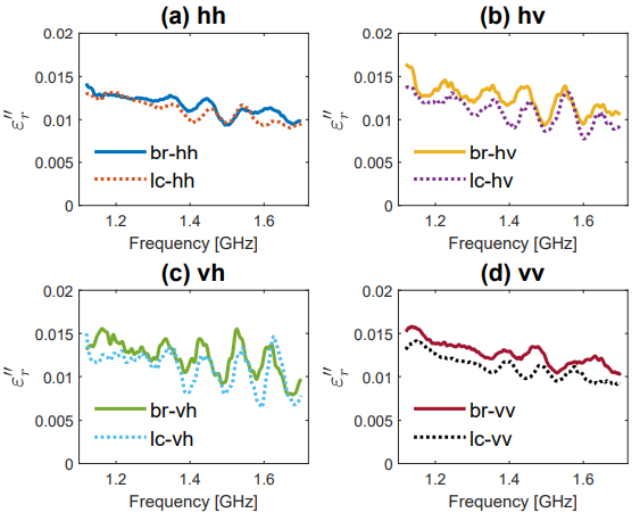


**Fig. 4** Frequency and polarization dependence of the calculated imaginary part of the complex permittivity, $\varepsilon_r''$.

## 5. Conclusions

The work demonstrated in this paper deals with the complex relative permittivity of typical construction walls in Southeast Asia, such as hollow clay brick (br) and lightweight concrete (lc). The measurement procedure is based on the propagation in free space conditions and through a slab of material for radiated measurement of an insertion transfer function for hh, hv, vh, and vv polarizations. The measurement results were reported for the frequency range from 1.12 GHz to 1.7 GHz, offering material-dependent characteristics and frequency dependency. According to the average results, the relative permittivity of lightweight concrete is less than the relative permittivity of clay brick in both polarizations. Furthermore, the curve progression is linear at the frequency range between 1.2 - 1.4 GHz. These outcomes are informative in the through-wall radar application, particularly for Southeast Asia construction material. Further work will focus on material characterization over a wider frequency band and more complex material in an urban environment.

## References

[1] S. Stavrou and S. R. Saunders, "Review of constitutive parameters of building materials," *Proc. of the 12th International Conference on Antennas and Propagation (ICAP 2003), Exeter, UK, 2003*, pp. 211-215 vol.1, doi: 10.1049/cp:20030052.

[2] D. Ferreira, I. Cuiñas, R. F. S. Caldeirinha and T. R. Fernandes, "A review on the electromagnetic characterisation of building materials at micro- and millimetre wave frequencies," *Proc. of the 8th European Conference on Antennas and Propagation (EuCAP 2014), The Hague, Netherlands, 2014*, pp. 145-149, doi: 10.1109/EuCAP. 2014.6901713.

[3] H. Okamoto, K. Kitao and S. Ichitsubo, "Outdoor-to-Indoor Propagation Loss Prediction in 800-MHz to 8-GHz Band for an Urban Area," *IEEE Transactions on Vehicular Technology*, vol. 58, no. 3, pp. 1059-1067, March 2009, doi: 10.1109/TVT.2008.927 996.

[4] J. Lu, D. Steinbach, P. Cabrol, P. Pietraski and R. V. Pragada, "Propagation characterization of an office building in the 60 GHz band," *Proc. of the 8th European Conference on Antennas and Propagation (EuCAP 2014), The Hague, Netherlands, 2014*, pp. 809-813, doi: 10.1109/EuCAP.2014.6901885.

[5] P. Protiva, J. Mrkvica, J. Machac, "Time delay estimation of UWB radar signals backscattered from a wall," *Microwave and Optical Technology Letters*, vol. 53, no. 6, pp. 1444-1450, 2011.

[6] S. S. Zhekov, O. Franek and G. F. Pedersen, "Dielectric Properties of Common Building Materials for Ultrawideband Propagation Studies [Measurements Corner]," *IEEE Antennas and Propagation Magazine*, vol. 62, no. 1, pp. 72-81, Feb. 2020, doi: 10.1109/MAP.2019.2955680.

[7] D. K. Ghodgaonkar, V. V. Varadan and V. K. Varadan, "A free-space method for measurement of dielectric constants and loss tangents at microwave frequencies," *IEEE Transactions on Instrumentation and Measurement*, vol. 38, no. 3, pp. 789-793, June 1989, doi: 10.1109/19.32194.

[8] S. Pisa, E. Pittella, E. Piuzzi, P. D'Atanasio and A. Zambotti, "Permittivity measurement on construction materials through free space method," *Proc. of the IEEE International Instrumentation and Measurement Technology Conference (I2MTC), Turin, Italy, 2017*, pp. 1-4, doi: 10.1109/I2MTC.2017.7969867.

[9] F. Sagnard and G. E. Zein, "In situ characterization of building materials for propagation modeling: frequency and time responses," *IEEE Transactions on Antennas and Propagation*, vol. 53, no. 10, pp. 3166-3173, Oct. 2005, doi: 10.1109/TAP.2005.856333.

[10] J. Ren, S. Chai and W. Chen, "Modeling the UWB through-the-wall signal pathloss measurements and Time Domain Ray tracing method," *Proc. of the IEEE International Conference on Microwave Technology & Computational Electromagnetics, Beijing, China, 2011*, pp. 334-337, doi: 10.1109/ICMTCE.2011.5915526.

[11] International Telecommunication Union (ITU). Recommendation ITU-R P.2040-2. Effects of building materials and structures on radiowave propagation above about 100 MHz. International Telecommunication Union; 2021. [Online]. Available: www.itu.int/rec/R-REC-P.2040-2-202109-I/en [Accessed Dec. 29, 2022].

[12] C.A. Balanis, *Advanced engineering electromagnetics*. New York, USA: John Wiley & Sons, 1989.

[13] H. Mott. *Remote Sensing with polarimetric radar*. USA: John Wiley & Sons, Inc., 2007.

[14] D. Pena, R. Feick, H. D. Hristov and W. Grote, "Measurement and modeling of propagation losses in brick and concrete walls for the 900-MHz band," *IEEE Transactions on Antennas and Propagation*, vol. 51, no. 1, pp. 31-39, Jan. 2003, doi: 10.1109/TAP.2003.808539.

[15] A. Asp, Y. Sydorov, M. Valkama and J. Niemelä, "Radio signal propagation and attenuation measurements for modern residential buildings," *Proc. of the IEEE Globecom Workshops, Anaheim, CA, USA, 2012*, pp. 580-584, doi: 10.1109/GLOCOMW.2012.6477638.

[16] I. Rodriguez, H. C. Nguyen, N. T. K. Jorgensen, T. B. Sorensen and P. Mogensen, "Radio Propagation into Modern Buildings: Attenuation Measurements in the Range from 800 MHz to 18 GHz," *Proc. of the IEEE 80th Vehicular Technology Conference (VTC2014-Fall), Vancouver, BC, Canada, 2014*, pp. 1-5, doi: 10.1109/VTCFall.2014.6966147.

[17] I. Cuinas and M. G. Sanchez, "Building material characterization from complex transmissivity measurements at 5.8 GHz," *IEEE Transactions on Antennas and Propagation*, vol. 48, no. 8, pp. 1269-1271, Aug. 2000, doi: 10.1109/8.884501.

[18] E. Greenberg and G. Segal, "Wall Parameters Sensitivity for Indoor Radio Waves Attenuation," *Proc. of the 14th European Conference on Antennas and Propagation (EuCAP), Copenhagen, Denmark, 2020*, pp. 1-5, doi: 10.23919/EuCAP48036.2020.9135748.

[19] M.G. Amin, *Through the wall radar imaging*. New York, USA: CRC Press, 2011.

[20] N. Iya, A. Muqaibel, U. Johar and M. A. Landolsi, "Ultra-wideband characterization of obstructed propagation," *Proc. of the 7th International Wireless Communications and Mobile Computing Conference, Istanbul, Turkey, 2011*, pp. 624-629, doi: 10.1109/IWCMC.2011.5982618.

[21] V. N. Saxena and R. Kaushik, "Characterization of Wall Parameters using Insertion Transfer Function Method in 'Through-the-Wall' Imaging System," *Proc. of the International Conference on Signal Processing and Communication (ICSC), NOIDA, India, 2019*, pp. 90-93, doi: 10.1109/ICSC45622.2019.8938351.

[22] A. H. Muqaibel and A. Safaai-Jazi, "A new formulation for characterization of materials based on measured insertion transfer function," *IEEE Transactions on Microwave Theory and Techniques*, vol. 51, no. 8, pp. 1946-1951, Aug. 2003, doi: 10.1109/TMTT.2003.815274.

[23] G. Tesserault, N. Malhouroux and P. Pajusco, "Determination of Material Characteristics for Optimizing WLAN Radio," *Proc. of the European Conference on Wireless Technologies, Munich, Germany, 2007*, pp. 225-228, doi: 10.1109/ECWT.2007.4403987.

[24] J. Ahmadi-Shokouh, S. Noghanian and H. Keshavarz, "Reflection Coefficient Measurement for North American House Flooring at 57–64 GHz," *IEEE Antennas and Wireless Propagation Letters*, vol. 10, pp. 1321-1324, 2011, doi: 10.1109/LAWP.2011.2177058.

[25] A. DiCarlofelice, E. DiGiampaolo, M. Feliziani and P. Tognolatti, "Experimental Characterization of Electromagnetic Propagation Under Rubble of a Historic Town After Disaster," *IEEE Transactions on Vehicular Technology*, vol. 64, no. 6, pp. 2288-2296, June 2015, doi: 10.1109/TVT.2014.2346580.

[26] D. Ferreira, R. F. S. Caldeirinha, T. R. Fernandes and I. Cuiñas, "Hollow Clay Brick Wall Propagation Analysis and Modified Brick Design for Enhanced Wi-Fi Coverage," *IEEE Transactions on Antennas and Propagation*, vol. 66, no. 1, pp. 331-339, Jan. 2018, doi: 10.1109/TAP.2017.2772028.

## Biographies

Narathep Phruksahiran received Dipl.-Ing. in Electrical Engineering and Information Technology from the University of the German Federal Armed Forces, Munich, Germany, in 2003 and Dr.-Ing. in Electrical Engineering and Information Technology from the Chemnitz University of Technology, Chemnitz, Germany, in 2013. He is an Associate Professor in the Department of Electrical Engineering at Chulachomklao Royal Military Academy, Nakhon-Nayok, Thailand. His research interests are in spectrum sensing and radio wave propagation.